# Study on Train Wheel Out-of-Roundness Monitoring Method by PVDF Sensing Technology

Ying Song*,[1], Zhichen Wang[1] and Yanliang Du[2]

[1]School of Transportation Institute, Shijiazhuang Tiedao University, Shijiazhuang 050043, China
[2]Structural Health Monitoring and Control Institute, Shijiazhuang Tiedao University, Shijiazhuang 050043, China

**Abstract:** Wheel out-of-roundness (OOR) inevitably jeopardizes the safety of railway operations. Regular visual inspection and checking by experienced workers are the commonly adopted practices to identify wheel defects. However, the defects may not be spotted timely. The paper puts forward a new method of real-time monitor wheel OOR based on PVDF strain sensor. In this method, the track strain response upon wheel-rail interaction is measured and processed to generate a condition index which directly reflects the wheel condition. Firstly, theoretical model of relationship between PVDF sensor output and wheel/rail loads was set up, and the principle for measuring vertical wheel/rail contact forces was proposed. Secondly, the effects of horizontal wheel/rail force and train speed on the output results have been discussed. Finally, this approach was verified by finite element analysis, and the preliminary results showed that this electromagnetic-immune system provides an effective alternative for wheel defects' detection.

**Keywords:** High-speed railway, non-roundness railway wheels, PVDF piezoelectric sensing, wheel/rail contact force measurement.

## 1. INTRODUCTION

Wheel condition monitoring is one of the critical features to ensure safe and cost-effective train operation in the railroad transportation industry. Nowadays, railway operators usually detect wheel defects by visual checking with experienced workers on a regular basis. Passengers' complaints or driver's report on excessive vibration is another means of identifying wheel defects. Moreover, periodical scheduled wheel re-profiling according to engineering experiences without defects' identification is also employed. These methods are useful in general but they do not guarantee on-time identification of wheel defects.

Thus, in order to minimize the costs for repair and maintenance and to meet noise legislation, there is a large economic incentive for real-time train wheel condition monitoring and removing out-of-round wheels before they can cause further damage. Many studies have been conducted to realize wheel defect detection and most of them are based on the analysis of wheel-rail interaction. Attivissimo *et al*. used a laser diode and a CCD camera to measure wheel and rail head profiles to evaluate the wheel-rail interaction quality [1]. However, the system was unable to discover the defects of wheel or rail. In addition, the laser source and camera required precision setup which is difficult for practical railroad application. Strain gauges and accelerometers were employed to measure the vertical wheel-rail contacting force and track response [2, 3]. Since the sensitivity of the system is relatively low, only the wheels with local defects of 0.5m in length can be identified. Sensors based on ultrasonic [4] and acoustic [5] techniques have also been employed to measure the wheel and rail conditions, but the performance of these sensors is easily compromised under electromagnetic interference (EMI) railroad environment. Besides, EMI free fiber optics sensor [6] has been used to detect flat wheels of train. However, other types of defects such as local spall or polygonal wheel cannot be retrieved.

This paper, proposed a new method based on PVDF strain sensor. Based on the response of wheel-rail contact forces due to OOR derived from numerical simulations, the sensors were used to measure the rail strain response upon wheel-rail interaction and the frequency component that solely reveals the quality of the interaction was extracted from the signal and processed in order to deduce the defects of passing wheels. The advantages of this sensor system are that both the sensors and measurement equipments installed at the railroad side are passive to EMI and non-zero drift. This feature is particularly favorable to the modern electrified railway system since the sensing network is immune from EMI. In addition, the method allows in-service and real-time monitoring of wheel condition, which is beneficial to the railway industry.

## 2. MEASURING METHOD

### 2.1. Measurement Scheme

In order to timely detect the wheel OOR , it is important to grasp the actual state of the contact forces between the wheel and rail. There are two kinds of measuring method based on PVDF piezoelectric sensing technology, i.e., "on-

*Address correspondence to this author at the School of Transportation Institute, Shijiazhuang Tiedao University, Shijiazhuang 050043, China;
Tel: 0086-311-87936613; Fax: 0086-311-87935038;
E-mail: sjzyingsong@sohu.com

1874-155X/14 2014 Bentham Open

board measuring" and "wayside inspection". "On-board measuring" uses "specially designed wheel sets", but there are interference signals caused by vibration, resulting in lower signal to noise ratio. A new method introduced in this paper uses "wayside measuring". In this method, PVDF sensors are attached on the rail web, and the contact forces are calculated from the measured changes in the strain of the rail web. It can examine the whole vehicles that run through measuring point because no equipment is required on vehicles, but only at specified points. Sketch of work principle is shown in Fig. (**1**).

### 2.2. Principle of Measuring Method

Taking the right rail as an example, the mechanical sketch of rail for single span is shown in Fig. (**2**), where $P$ and $Q$ are vertical and horizontal wheel/rail forces respectively. $F_{h1}$ , $F_{h2}$ , $F_{v1}$ and $F_{v2}$ are reaction forces at sleepers. Stresses along longitudinal direction (*i.e.*, $z$ direction) at point 1 and point 2 are obtained as

$$\begin{cases} \sigma_{1z} = \sigma\left(M_{x,1-2}\right) - \sigma\left(M_{y,1-2}\right) - \sigma\left(T_{z,1-2}\right) \\ \sigma_{2z} = \sigma\left(M_{x,1-2}\right) + \sigma\left(M_{y,1-2}\right) + \sigma\left(T_{z,1-2}\right) \end{cases} \tag{1}$$

where $M_{x,1-2}$ and $M_{y,1-2}$ are moments on cross section 1-2 about the $x$ axis and the $y$ axis respectively, and $T_{z,1-2}$ is the torque about $z$ axis at section 1-2. $M_{x,1-2}$ , $M_{y,1-2}$ , and $T_{z,1-2}$ can be obtained as

$$\begin{cases} M_{x,1-2} = F_{v1} \cdot l = \left(P/2\right) \cdot l \\ M_{y,1-2} = F_{h1} \cdot l \\ T_{z,1-2} = P \cdot \delta - Q \cdot h \end{cases} \tag{2}$$

From Eq.(1) and Eq.(2), following equation is obtained:

$$\begin{aligned} \sigma_{1z} + \sigma_{2z} &= 2 \cdot \sigma\left(M_{x,1-2}\right) \\ &= 2\frac{\left(P/2\right) \cdot l}{I_x} \cdot a = C \cdot P \end{aligned} \tag{3}$$

Where $C$ is constant which depends on material properties and geometrical size of the rail. Thus, if strain is measured along longitudinal direction at point 1 and point 2, the vertical wheel/rail force $P$ can be calculated. Based on the basic piezoelectric equations, the relationship between measured strain and output signal generated by PVDF sensing element is as follows: (external electric field is zero as PVDF piezoelectric film being used as a sensor)

$$D_i = d_{ij} T_j \left(i = 1 \sim 3, j = 1 \sim 6\right) \tag{4}$$

where $D_i\left(i = 1 \sim 3\right)$ denotes the electric displacement, $d_{ij}\left(i = 1 \sim 3, j = 1 \sim 6\right)$ denotes the piezoelectric constant, and $T_j\left(j = 1 \sim 6\right)$ is the stress applied on the sensing element.

For PVDF piezoelectric film, $d_{31} = d_{32}$ , $d_{24} = d_{15}$ , and other piezoelectric constants are zero. The output signal of PVDF sensor is induced by strains in all directions. For wheel/rail force measurement, according to Figs. (**1**, **2**), the output signal is induced only by the strain in single direction, and the electric displacement is along the direction of $D_3$. The output charge of PVDF sensing element can be expressed as,

$$Q = D_3 S_p = d_{31} T_1 S_p = d_{31} E_{pvdf} S_1 S_p \tag{5}$$

where, $S_p$ is the affect area of PVDF polar plate, $E_{pvdf}$ is the Elastic Modulus and $S_1$ is the measured strain. In practical engineering application, a charge amplifier is required to convert the charge signal into voltage signal, which is then converted into the digital signal by A/D converter, to form a fully automated monitoring system combining them with data acquisition, processing and analysis software. Assume that $K_A$ is a proportional coefficient of charge amplifier, $A_b$ is an amplification factor of post-processing circuit, the output voltage of the whole circuit can be given by:

$$U_o = K_A d_{31} E_{pvdf} S_1 S_p A_b \tag{6}$$

In this way, once parameters of PVDF sensor element and circuit are known, the values of the generated charge can be measured, and the vertical and horizontal wheel/rail force can then be obtained using Eqs.(3) and (6).

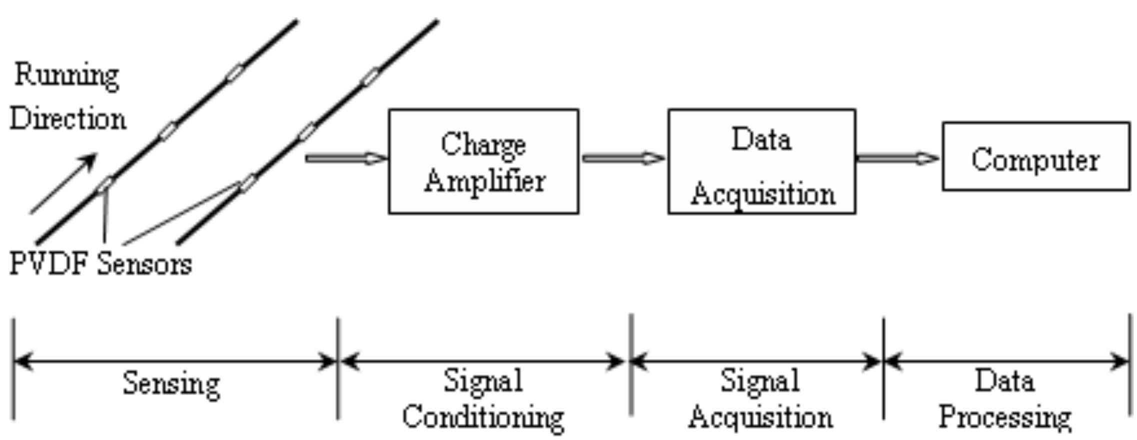


**Fig. (1).** Sketch of work principle.

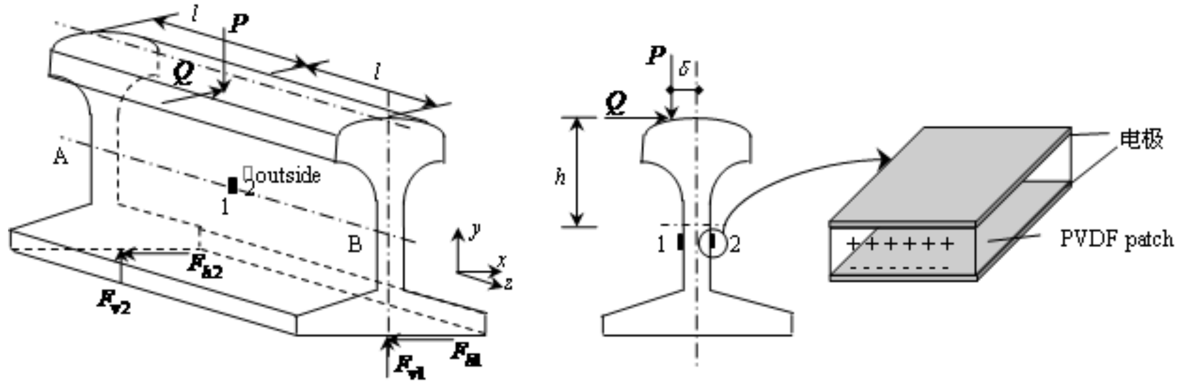


**Fig. (2).** Mechanical sketch of rail for single span.

### 2.3. Analysis and Validation

A FEM (Finite Element Method) model was developed for calculating the surface stress/strain of rail under vertical and lateral wheel/rail contact forces. The discretely supported 60kg/m rail was modeled by solid element. The length of the track model was 8 sleeper bays with a constant sleeper spacing of 568mm and the boundaries at the two rail ends were supported. Each rail pad was modeled as a discrete linear elastic spring. Ballast and subgrade were modeled by solid elements. Train load was modeled by concentrated loading. Load cases are shown in Table **1**.

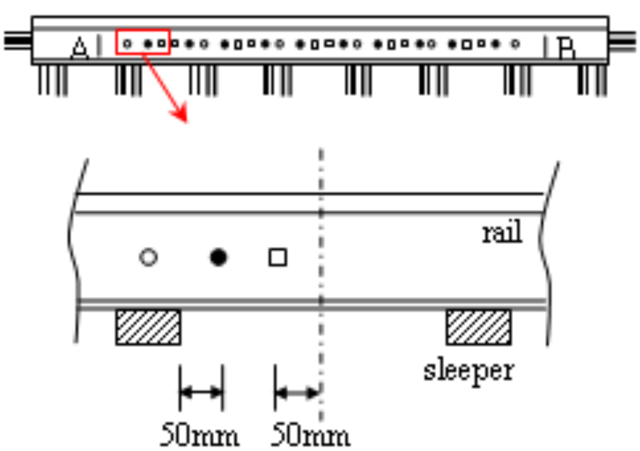


**Fig. (3a).** Sketch of sensor locations in simulation calculation.

Based on Case 1 as shown in Table **1**, horizontal wheel/rail force and train speed were kept constant. The relationship between ($\sigma_{1z}+\sigma_{2z}$) (see Eq.(3)) and vertical wheel/rail force *P* located in different strain measuring points (*i.e.*, at the end of a sleeper bay, away from mid-span of a sleeper bay 50mm and away from sleeper end 50mm) is shown in Fig. (**3**). The constant "*C*" as shown in Eq.(3) was calculated by slope of the curve, and the slope was kept constant with the change in vertical forces. Slope of the curve in "Location 3" was greater than that in "Location 1" and "Location 2". Location 3 (away from sleeper end 50mm) was observed as a reasonable paste position of the PVDF strain sensor, and the measuring point was strain-sensitive. Following this, vertical wheel/rail force was calculated from Eq.(3) and Eq.(6). The numerical results agree well with theoretical analysis.

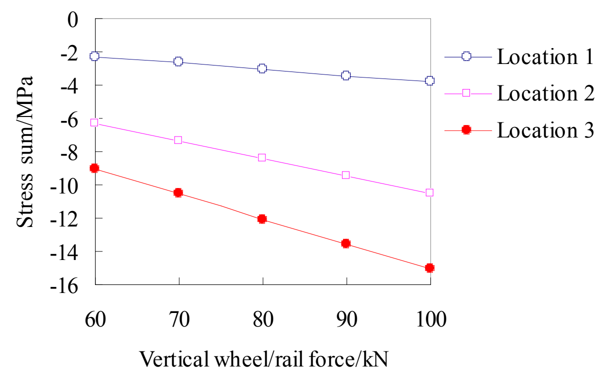


**Fig. (3b).** Relationship of stress *versus* vertical wheel/rail force.

Based on Case 2 as shown in Table **1**, vertical wheel/rail force and train speed were kept constant. Simulation results at different horizontal wheel/rail forces showed that the horizontal wheel/rail force had insignificant effect on slope of the measured curve, as shown in Fig. (**4**).

Based on Case 3 as shown in Table **1**, for given unchanged vertical wheel/rail force , simulation results at different train velocities showed that train velocity has insignificant effect on slope of the measured curve, as shown in Fig. (**5**). It was concluded that vertical wheel/rail force can be calculated from Eq.(3) and Eq.(6).

**Table 1. Load cases of simulation.**

| Load Case | Vertical Wheel/Rail Force [kN] | Horizontal Wheel/Rail Force [kN] | Train Speed [km/h] |
|---|---|---|---|
| 1 | 60, 70, 80, 90, 100 | 0 | 200 |
| 2 | 80 | 30, 40, 50, 60, 70 | 200 |
| 3 | 80 | 0 | 200, 250, 300, 350 |

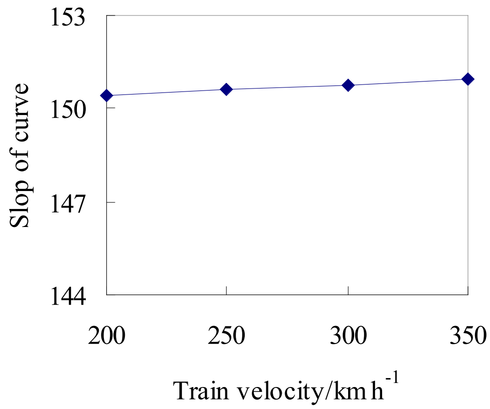


**Fig. (4).** Curve slope *versus* speed.

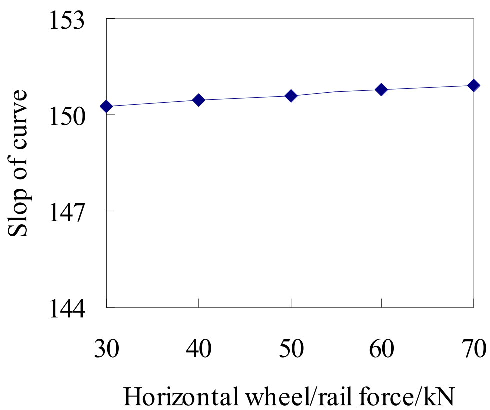


**Fig. (5).** Curve slope *versus* horizontal wheel/rail force.

In the study [7] and [8], the influence on dynamic response of wheel/rail impact vibration due to OOR derived from simulations was systematically studied, and the relationship between safety threshold of wheel OOR and vehicle speed was set up. Hence, train wheel condition using PVDF sensors to measure the track strain response upon wheel-rail interaction can be detected timely.

## CONCLUSION

Research on wheel/rail force real-time monitoring technology under OOR excitation is of great significance to ensure safe operation of high-speed railway and to improve ride comfort. Combined with the characteristic of wheel/rail interaction force under OOR excitation, theoretical model and Finite Element Model of relationship between PVDF sensor output and wheel/rail loads were set up with the principle for measuring vertical wheel/rail contact force. The method was verified by FEM simulation. Further tests and verifications with wheel and rail condition data are still required to ensure the long-term reliability of the proposed method. To improve the measurement accuracy and overall integrity of the system, a more intelligent analysis technique is currently under investigation.

## CONFLICT OF INTEREST

The authors confirm that this article content has no conflict of interest.

## ACKNOWLEDGEMENTS

This research was supported by the National Nature Science Foundation of China (Grant No. 51208318, 11372199, 51208319), as well as by the Hebei Province Natural Science Foundation (Grant No. E2011210032) and the Educational Scientific Research Project of Hebei Province (Grant No. Q2012025, ZD2010110).

## REFERENCES

[1] J.B. Meng, W.J. Xu, and W.Q. Song, “Modelling of reactive kinetics in the metal surface contaminant cleaning using atmospheric pressure plasma arc”, *Appl. Surf. Sci.*, vol. 254, pp. 6826-6830, 2008.

[2] F. Attivissimo, A. Danese, N. Giaquinto, and P. Sforza. “A railway measurement system to evaluate the wheel-rail interaction quality”, *IEEE Trans. Instrum. Meas*., vol. 56, pp. 1583-1589, 2007.

[3] A. Johansson, and J.C.O. Nielsen, “Out-of-round railway wheels-wheel-rail contact forces and track response derived from field tests and numerical simulations”, *IMechE J. Rail Rapid Transit.*, vol. 217, pp. 135-145, 2003.

[4] A. Johansson, “Out-of-round railway wheels-assessment of wheel tread irregularities in train traffic”, *J. Sound Vib*., vol. 293, pp. 795-806, 2006.

[5] M. Guagliano, and M. Pau, “An experimental-numerical approach for the analysis of internally cracked railway wheels”, *Wear*, vol. 265, pp. 1387-1395, 2008.

[6] E. Matzan, “*System for Detection of Defects in Railroad Car Wheels*”, U.S. Patent 7213789, 2007.

[7] D.R. Anderson, “Detecting flat wheels with a fiber-optic sensor”, JRC’06, April 4-6, 2006, Atlanta, Georgia, pp. 25-30, 2006.

[8] Y. Song, and Z.C. Wang, “Research on the control of out-of-round wheel profiles of high-speed railway derived from numerical simulations”. *Int. J. Online Eng.,* vol. 9, pp. 92-95, 2013.

Received: November 11, 2013 Revised: February 11, 2014 Accepted: March 3, 2014